Raman Longitudinal Acoustic Mode (LAM) Studies of Folded-Chain Morphology in Poly(ethylene oxide) (PEO). 3. Chain Folding in PEO as a Function of Molecular Weight

Kigook Song† and Samuel Krimm*

Macromolecular Research Center and Department of Physics, The University of Michigan, Ann Arbor, Michigan 48109. *Received June 16, 1989*

ABSTRACT: We have obtained Raman LAM spectra for a series of PEO fractions crystallized under different conditions and have interpreted these with the aid of results from normal mode calculations. Our LAM, X-ray, and DSC data indicate the existence of folded-chain structures more complex than the previously proposed simple integer-fold lamellae. We find evidence for lamellae consisting of once-folded chains in bilayer arrangements, for lamellae containing mixed integer-fold structures, and for lamellae based on half-integer-fold chains. The once-folded bilayer structures provide a mechanism for transformation, by reptation, to fully extended chains, and we see evidence in the LAM spectra for intermediate stages in this conversion.

Introduction

A quantized increase of lamellar thickness with crystallization temperature has been reported for low molecular weight fractions of PEO in small-angle X-ray scattering (SAXS) studies by Spegt and co-workers.[1-3] Such a stepwise transition in PEO crystals has also been observed by studies of crystal growth rate using optical microscopy[4-7] and by differential scanning calorimetry (DSC) studies.[8,9] These observations indicate that PEO chains have a tendency to fold in integral reciprocals of the extended-chain length. This has led to the concept of integer folds (IF) in these systems, viz., molecules for which all stems are of the same length with chain ends located at the lamellar surfaces. Similar IF structures have been proposed for monodisperse ultralong *n*-paraffins.[10]

In all of the above PEO studies it has been assumed that, for a given polymer and crystallization condition, the lamellae are homogeneous and contain only single IF structures. This assumption was also made for bilayer crystals, i.e., double lamellae, observed by optical[7] and transmission electron microscopy,[11] that are composed of chains with an odd number of folds. Our studies on PEO suggest that there are lamellae that contain a mixture of IF structures, as well as lamellae that contain chains with simple fractional-integer folds (FIF). These conclusions are a consequence of combining the inferences from SAXS and DSC data with the results of longitudinal acoustic mode (LAM) studies, a spectroscopic technique that can reveal morphological features not accessible to the former two methods. We believe that such FIF are also indicated by results on ultralong *n*-paraffins,[12,13] although the SAXS data were interpreted[13] in terms of general noninteger folds.

The first-order LAM frequency ν (LAM-1 or LAM) can be used to determine the ordered length, L, of a polymer chain stem in a crystalline lamella. However, the value obtained for L depends on the assumptions made in relating ν to L: for an unperturbed elastic rod model, $\nu = (1/2L)(E/\rho)^{1/2}$, where E is the elastic modulus and ρ is the density of the rod; for the general perturbed composite elastic rod, more complex relationships hold;[14,15] and if the polymer stem is treated at a molecular rather than a continuum level, the detailed effects of perturbations can be elucidated only by normal-mode analyses.[16]

In order to provide a rigorous interpretation of the LAM results on PEO, we have refined a force field that includes intermolecular interactions explicitly[17] and have used it in normal-mode calculations of the LAM of helical-chain oligomers[17] and of models of folded-chain structures.[18] In the present studies, the results of such normal-mode analyses are employed to interpret Raman LAM spectra of a series of PEO fractions crystallized under different conditions. These results are combined with SAXS and DSC experiments to provide a more detailed view of the morphologies of these samples, resulting in the conclusions mentioned above (about which a preliminary communication has appeared[19]). After presenting our experimental methods and reviewing some results of our normal-mode calculations, we discuss the results and conclusions for each fraction. The order of discussions is chosen so as to present what we feel is the clearest development of understanding of the LAM spectra and of the structures in this semicrystalline polymer.

Table I
Molecular Parameters of PEO Samples

sample designatn	M_n, g/mol	M_w/M_n	calcd chain length, Å	X_H
1000	1007	1.05	64	0.77
1500	1423	1.05	90	0.81
2000	1967	1.05	124	0.85
3000	3336	1.10	211	0.89
5000	4506	1.10	285	0.90

Experimental Section

Materials. The PEO samples used in this study were hydroxy-terminated low molecular weight fractions obtained from Scientific Polymer Products, Inc. All samples were used without further purification. The molecular weights and molecular weight distributions of each fraction are listed in Table I. The extended-chain length, i.e., the length along the helical-chain axis, was calculated from crystallographic dimensions of the PEO 7_2 helix[20] and is tabulated in Table I. The following formula is used to obtain the theoretical chain length, L.

$$L\ (\text{Å}) = \frac{M_n}{44}\frac{19.48}{7} \quad (1)$$

For stem lengths of a folded chain, three chemical repeat units

† Present address: IBM Almaden Research Center, San Jose, CA 95120.

0024-9297/90/2223-1946$02.50/0

are assumed for each fold, and thus 8.3 Å/fold was subtracted from the extended-chain length before dividing by the number of stems.

Each sample was contained in a thin glass capillary, flushed with argon, and the capillary sealed by flame. The specimens were melted in an oven and then isothermally crystallized for specified times at various temperatures (T_c) in a water bath. The self-seeding technique[21] was employed for specimens crystallized near the melting temperature in order to reduce crystallization times.

Raman Spectroscopy. Raman spectra were obtained with a Spex 1403 double monochromator equipped with holographic gratings and a Spectra Physics 165 argon ion laser operated at 514.5 nm and 300 mW. In order to reduce stray light from Rayleigh scattering, a Spex 1442 third monochromator was added so that the range of observation of the spectra could be extended down to 3 cm^{-1}. The spectra were run at very low scan speeds (<0.03 cm^{-1}/s) with a resolution of 1.5 cm^{-1} (the step resolution being 0.1 cm^{-1}). Pure rotational Raman bands due to air (nitrogen and oxygen) were observed in the low-frequency region from an empty glass capillary. These bands[22] were used to calibrate the spectrometer in this region, and thus the measurement error was kept to less than ±0.1 cm^{-1}. During the scan of a sample, argon gas was passed over the capillary to remove these air bands from the spectrum.

Spectra were generally obtained at room temperature, but some specimens were studied at reduced temperature using a dry ice/acetone mixture in a low-temperature cell. Frequency and temperature corrections[23] were applied to some spectra, but the changes in the frequency at the peak due to such corrections were found to be negligible for the narrow LAM bands of PEO, whose half-widths are usually less than 2 cm^{-1}, and such corrections were therefore not generally used.

Differential Scanning Calorimetry. A Perkin-Elmer DSC-7 differential scanning calorimeter was used to study the melting behavior of different fractions of PEO. The temperature scale of the calorimeter was calibrated using naphthalene. The same specimens used in the Raman experiment were employed for DSC measurements. Less than 1 mg of the sample was melted to reduce thermal inertia of the specimen. Unless otherwise noted, DSC thermograms reported in the present study were recorded at a heating rate of 5 °C/min.

From the measured heats of fusion, ΔH_f, a degree of crystallinity, X_H, was determined from $X_H = \Delta H_f/\Delta H_f°$, where $\Delta H_f°$ (the heat of fusion of perfectly crystalline PEO) was calculated from the melting point.[24] These values are listed in Table I. Using a fixed value of $\Delta H_f°$ [8,9] gives X_H values that are slightly higher, 0.78 for PEO 1000 to 0.95 for PEO 5000.

X-ray Diffraction. SAXS data were obtained at room temperature using an Elliot GX-20 rotating anode X-ray generator with Cu Kα radiation, of wavelength 1.54 Å. The sample to detector distance was 90 cm. One-dimensional position-sensitive detection was used with exposure times of about 6 h for each sample. The sample was sealed in a thin-walled glass X-ray capillary of 1-mm diameter and melt-crystallized in a water bath. Bragg's law was used to obtain the spacings. No corrections were made to the observed X-ray diffraction patterns.

Normal-Coordinate Analysis

Normal-mode calculations were carried out for extended-chain PEO molecules up to a 53-mer (MW = 2350 g/mol) with our refined intra- and interchain force fields.[17] The calculated LAM frequencies with longitudinal hydrogen bonds at chain ends and without such end interactions[25] give straight lines in both cases when they are plotted against the reciprocal chain length (Figure 1). The difference between the two lines, which reflects the end force perturbations due to hydrogen bonding, is about 3 cm^{-1}. The observed extended-chain LAM frequencies are plotted against the reciprocal chain length and compared with these calculated relationships in Figure 1. The observed frequencies for monodisperse oligooxyethylenes[26] (35-mer, 25-mer, and 15-mer) agree well with the line representing the LAM frequencies calculated by including hydrogen bonding, whereas those for our polydisperse PEO samples fall between the lines (our observed data will be discussed in detail in the next section, together with their spectra). The end groups in monodisperse oligooxyethylenes are known[27] to be hydrogen bonded in end-group layers; in fact, the chain ends for the 9-mer and 15-mer are so well ordered that such oligomers do not give SAXS peaks.[24] Thus, the observed data for the monodisperse samples are consistent with the calculated results that include end force interactions. Polydisperse samples have lower LAM frequencies than monodisperse samples, probably because their irregular lamellar end surfaces result in fewer and weaker longitudinal hydrogen bonds. (Lateral hydrogen bonds between end groups of chains in the same lamella, which are more likely for polydisperse samples, are not expected to have as large an effect on the LAM frequency as longitudinal hydrogen bonds between chain ends in adjacent lamellae.) The results in Figure 1 indicate that the observed LAM frequencies for the polydisperse samples are close to the values calculated without longitudinal hydrogen bonds, and the effect of such hydrogen bonding becomes weaker as the molecular weight (and in fact the polydispersity) increases. The observed LAM frequencies for the polydisperse samples also fall on a straight line, so that an observed LAM frequency can be converted to a corresponding chain length by interpolation, using the appropriate curve.

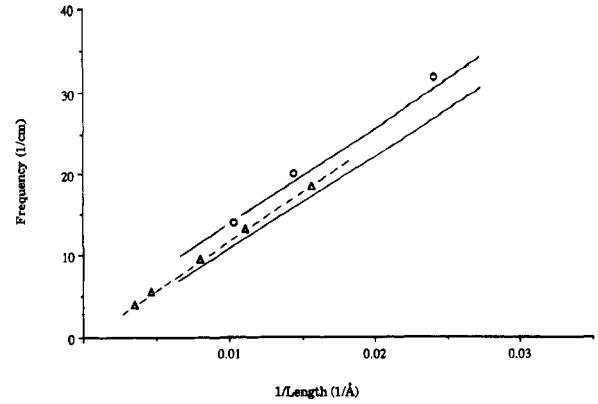

Figure 1. Observed LAM frequency of an extended chain of PEO versus reciprocal chain length: (○) 35-mer, 25-mer, and 15-mer; (△) PEO 5000, 3000, 2000, 1500, and 1000. Solid lines are obtained from normal-mode analyses of PEO representing the calculated LAM frequencies with hydrogen bonding (upper) and without hydrogen bonding (lower). Broken line denotes the observed LAM frequency of polydisperse samples.

The Raman spectra of higher molecular weight samples (≥PEO 3000) show multiple LAM bands that correspond to stem lengths of extended, once-folded, and multifolded chains. The observed LAM frequency of a once-folded chain is about twice that of an extended chain. The above frequency/chain length relation shows that the stem length of such a once-folded chain is about half that of an extended-chain length. This suggests that the fold is tight, comprising relatively few atoms, and therefore the chain folding must involve adjacent reentry. We also infer from the above frequency relation that the LAM frequency is not much affected by the presence of a fold, as we predicted in our previous study[18] based on the results of normal-coordinate analyses on model folded-chain molecules.

Results and Discussion

Extended-Chain PEO. PEO 2000. Low-frequency Raman spectra of PEO 2000 recorded at room tempera-

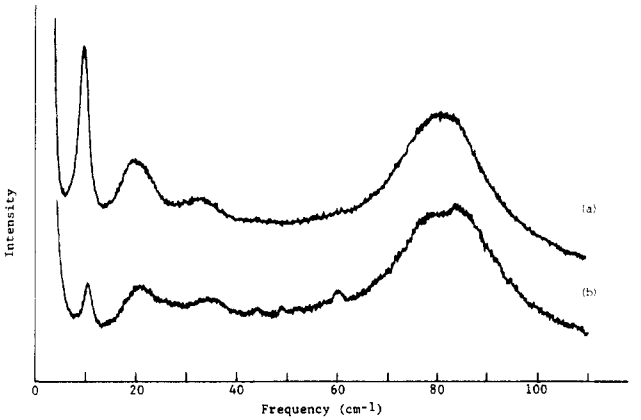

Figure 2. Low-frequency Raman spectra of PEO 2000 recorded at (a) RT and (b) −79 °C.

Table II
X-ray Spacings and Observed LAM Frequencies of PEO 1500 and PEO 2000[a]

	L, Å		
sample	calcd[b]	SAXS	LAM ν, cm^{-1}
1500	90	90	13.2
2000	124	125	9.5

[a] Room-temperature crystallized sample. [b] Obtained using eq 1.

ture and at dry ice/acetone temperature are shown in Figure 2. The intense scattering peak located at 9.5 cm^{-1} (Table II) in the room temperature spectrum has been assigned to the LAM of an extended PEO 2000 chain on the basis of the chain-length dependence of the peak frequency.[26] Our normal-mode calculation of an extended-chain molecule of PEO 2000 molecular weight also predicts about the same LAM frequency as that observed, ~9.0 cm^{-1} in the absence of hydrogen bond interactions (see Figure 1). The same type of spectrum was found at all crystallization temperatures investigated. As the sample temperature is decreased, the LAM band shifts to higher frequency (10.5 cm^{-1}) and decreases significantly in intensity. Both of these effects are specific to the LAM, being due to thermal contraction of the unit cell on cooling, and will be discussed in detail below with the results for other PEO samples.

Other than the LAM, three additional bands, near 80, 33.5, and 19.5 cm^{-1}, are observed in the room-temperature spectrum (the weak scattering peaks at 60 cm^{-1} and near 50 cm^{-1} in the low-temperature spectrum are the pure rotation Raman bands of air, which was not completely excluded in this case). These bands are found in the low-frequency spectra of all PEO samples, irrespective of chain length, and are therefore not associated with the LAM. Rabolt et al.[28] have assigned the peak at 80 cm^{-1} to a CO torsion mode of E symmetry species. Recently, Viras et al.[29] indicated that a lattice mode also contributes to scattering near 80 cm^{-1}. This is supported by the appearance of a second peak near 84 cm^{-1} in the low-temperature spectrum, the lattice mode, overlapping at 80 cm^{-1} at room temperature, shifting as expected to higher frequency at lower temperature. The bands at ~33.5 and 19.5 cm^{-1} in the room-temperature spectrum shift to higher frequencies, 35 and 21 cm^{-1}, respectively, at low temperature, shifts also found for other PEO samples. Although the band at 33.5 cm^{-1} is weak and broad, we believe on the basis of the temperature dependence of the frequency that this band is a lattice mode. The low-temperature frequency shift of the band at 19.5 cm^{-1} is quite obvious and indicates that it should

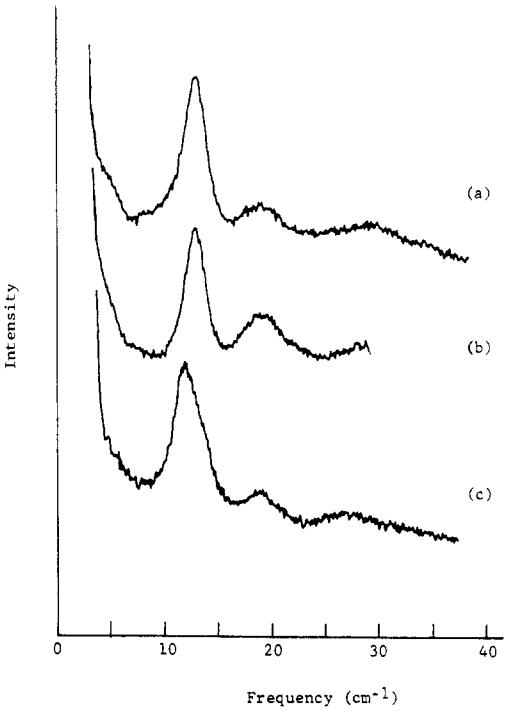

Figure 3. Low-frequency Raman spectra of PEO 1500 crystallized at different temperatures: (a) RT, (b) 34 °C, and (c) 44 °C.

be assigned to another lattice mode. It has been proposed[26] that this band is a third-order LAM (LAM-3), but its frequency and intensity behavior are inconsistent with such an assignment. The shoulder near 22 cm^{-1} is more reasonably assigned to the LAM-3 of PEO 2000: its intensity decreases at low temperature and its frequency ratio to the LAM is 2.3, which is in the range (2.3–2.6) derived for the frequency ratio of LAM-3 to LAM from our normal-mode calculations.[25] It should be noted that the intensity of the LAM-3 band is much lower than that of the LAM.

The lamellar periodicity measured by SAXS for this sample was 125 Å (see Table II). This value is close to the chain length calculated from the number-average molecular weight of the sample. The DSC thermogram of this sample shows only one endothermic peak at 54.5 °C, corresponding to the melting point expected of extended-chain crystals. Thus, the three techniques unambiguously show that PEO 2000 crystallizes in an extended-chain conformation with the helix axis normal to the lamellar end surfaces.

PEO 1500. A SAXS periodicity of 90 Å was obtained for PEO 1500, which is consistent with the calculated length of such an extended-chain molecule crystallized at room temperature (Table II). In Figures 3 and 4 are shown the Raman spectra and DSC thermograms, respectively, of samples crystallized at room temperature (RT), 34 °C, and 44 °C. The curves for the T_c = RT and T_c = 34 °C samples are the same. The intense band at 13.2 cm^{-1} and the melting peak at 48.4 °C are associated with the LAM of extended-chain molecules and the melting point of lamellae of such chains, respectively. The normal-mode calculations also indicate that the LAM band at 13.2 cm^{-1} corresponds to the length of an extended chain of PEO 1500, ~12.4 cm^{-1} in the absence of hydrogen bond interactions (see Figure 1). A weak and broad scattering peak near 30 cm^{-1} is observed in the Raman spectrum of the T_c = RT sample. This band is assignable to LAM-3 on the basis of the frequency ratio (LAM-

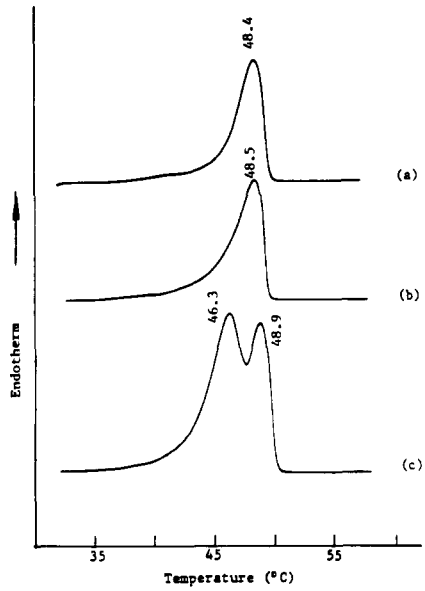

Figure 4. DSC melting curves of PEO 1500 crystallized at different temperatures: (a) RT, (b) 34 °C, and (c) 44 °C.

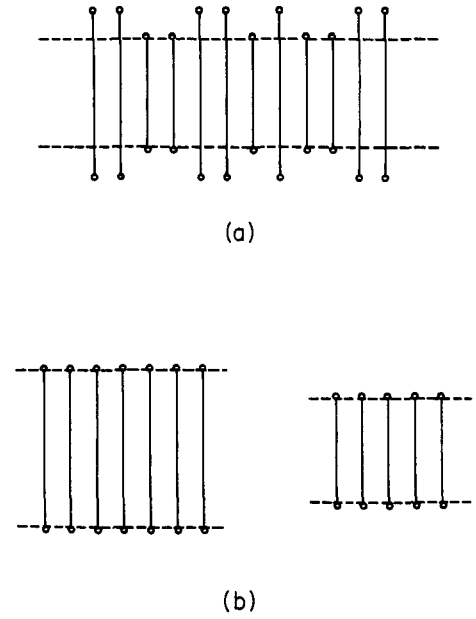

Figure 5. Schematic illustration of fractionation: (a) before fractionation, (b) after fractionation.

3/LAM) of 2.3, which is in the expected range for the LAM-3 mode. We will comment in the next section on the weak band near 6 cm^{-1} shown in Figure 3a.

For the T_c = 44 °C sample, the Raman spectrum (Figure 3c) shows a peak at 12.3 cm^{-1} and a weak band near 27.5 cm^{-1}. These two bands are assignable to LAM and LAM-3 modes, respectively. The frequencies of these bands are lower than those for the low T_c samples (parts a and b of Figure 3). It is known from our previous studies[16,17] that there are three main reasons for a decrease in a LAM frequency: (1) an increase in chain length; (2) a decrease in force perturbations, such as chain end and lateral interchain interactions; and (3) an increase in mass perturbations at chain ends. While disordered chain ends at the lamellar surface can act as additional masses perturbing the LAM, as found in our normal-mode analyses on folded-chain molecules,[18] it is unreasonable to expect an increase in such perturbations at higher crystallization temperature, since disorder at the chain ends should be reduced to give a more perfect crystal structure. By the same reasoning, an increase in force perturbations should occur at higher crystallization temperature. Thus, an increase in the LAM frequency, instead of the observed decrease, would be predicted for the T_c = 44 °C sample as a result of expected changes in mass and force perturbations. The remaining reason for the decrease in the LAM frequency, viz., an increase in the ordered stem length in the lamella, seems most consistent with the LAM frequency shift observed for the T_c = 44 °C sample. Our calculations show that the observed shift corresponds to an increase of 6 Å in the stem length, which is about the length of two chemical repeat units along the chain axis direction. Therefore, it might be thought that disordered chain ends of one unit length at each end become part of the lamellar stems at higher crystallization temperature.

However, this simple explanation cannot account for the DSC curve observed for the T_c = 44 °C sample, which shows two melting peaks of similar intensities (Figure 4c). All samples crystallized at low T_c give a single melting peak near 48.4 °C, but when crystallized at T_c = 44 °C, two melting peaks, at 46.3 and 48.9 °C, are observed. The presence of two melting peaks implies the existence of two types of lamellae of different thicknesses. It has been known from SAXS[30,31] and dilatometric investigations[4] that near the melting temperature low molecular weight fractions of PEO show fractionation during the crystallization process. Therefore, we believe that at T_c = 44 °C the PEO 1500 molecules become segregated by molecular weight into lamellae of different thicknesses. The LAM spectrum is expected to reflect such fractionation because each stem of different length gives a different frequency. Indeed, the LAM band at 12.3 cm^{-1} for the T_c = 44 °C sample is asymmetric and seems to overlap a band of frequency higher than 13.2 cm^{-1}.

To explain this behavior, we envision that, before fractionation, a distribution of chain lengths exists in a crystal (see Figure 5, which for simplicity shows two lengths). The pendent atoms of the longer chains do not experience the lateral interchain interactions that the atoms in the crystal do; in fact, the overhanging ends are probably disordered. Therefore, as shown in our previous study,[18] the effective chain length for determining the LAM frequency of the longer chain molecules in the mixed crystal is decreased and is the same as the length of the short-chain molecules. Thus, the LAM frequency of the mixed crystal effectively corresponds to the short-chain length, lowered slightly by the inertial contributions of the disordered chain ends.[18] After fractionation, longer and shorter chain molecules segregate and form their own crystals. The LAM band at 12.3 cm^{-1} and the shoulder at ~13.8 cm^{-1} found for the T_c = 44 °C sample thus correspond to the lamellae of the longer and the shorter chain molecules, respectively. This interpretation is consistent with the DSC melting curves. The peak at 48.4 °C for the low T_c samples is associated with the mixed crystals, and the peaks at 46.3 and 48.9 °C for the T_c = 44 °C sample correspond to fractionated short-chain and long-chain lamellae, respectively.

PEO 1000. Low-frequency Raman spectra for PEO 1000 samples crystallized at different temperatures are shown in Figure 6. Two bands are found, at 8.1 and 18.5 cm^{-1}, for the T_c = RT sample, and these bands shift to higher frequencies with increasing T_c (Table III). The lattice mode band expected at 19.5 cm^{-1} is not clearly seen, and we presume that it is overlapped by the 18.5-cm^{-1} band. If both observed bands were LAM bands, they would be attributable to different lamellar thicknesses in the sample. However, our SAXS data do not

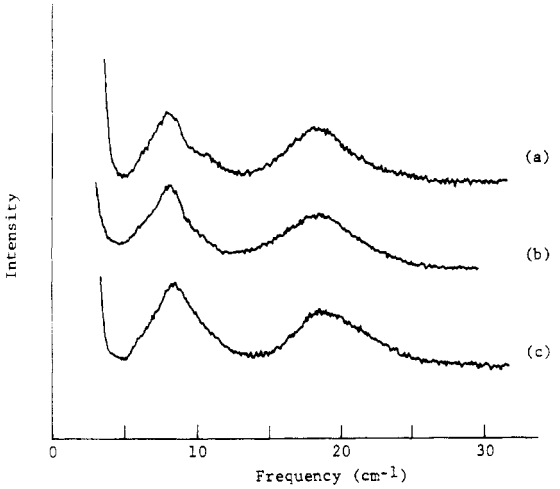

Figure 6. Low-frequency Raman spectra of PEO 1000 crystallized at different conditions: (a) RT, (b) 34 °C (2 days), and (c) 34 °C (7 days).

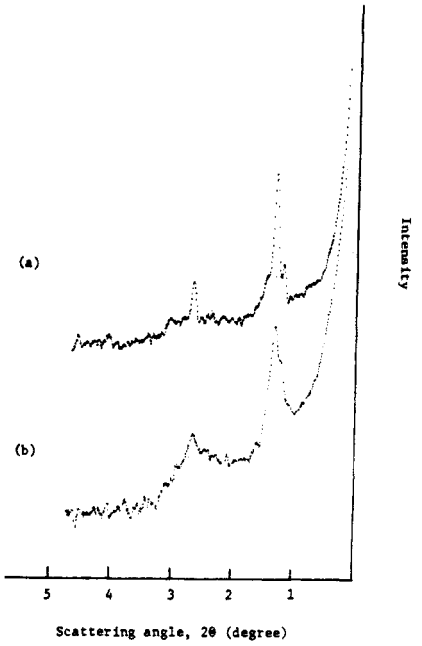

Figure 7. Small-angle X-ray diffraction patterns of PEO 1000 crystallized at different temperatures: (a) RT and (b) 34 °C (2 days).

Table III
X-ray Spacings, Observed LAM Frequencies, and Melting Points of PEO 1000

crystallizn				melting
temp, °C	time, days	SAXS L, Å	LAM ν, cm^{-1}	point, °C
RT	5	68	8.1/18.5	34.5/40.2
34	2	68	8.2/18.7	36.2/40.5
34	7		8.6/19.2	36.6/41.1

support this interpretation. The X-ray patterns shown in Figure 7 exhibit two orders of a single periodicity of 68 Å, suggesting one discrete lamellar thickness corresponding to the extended-chain length. Thus, the two bands shown in Figure 6 cannot be attributed to two distinguishable chain lengths.

The LAM frequency of a PEO 1000 molecule can be obtained from its theoretical chain length by using the curves in Figure 1. When the chain-end hydrogen bonds are included in the calculation, the predicted frequency is found to be 20.8 cm^{-1}; without such end interactions 17.5 cm^{-1} is obtained. It is therefore evident that the band at 18.5 cm^{-1}, which is in the calculated LAM frequency range, is assignable to the LAM of PEO 1000. Since the other band is at about half the LAM frequency, the chain length corresponding to it should be twice that of PEO 1000. Such (presumably dimeric) structures are not likely, and furthermore the corresponding X-ray spacing is not observed.

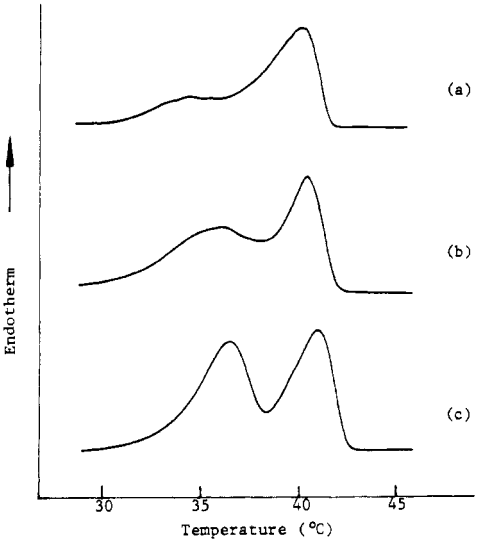

Figure 8. DSC melting curves of PEO 1000 crystallized at different conditions: (a) RT, (b) 34 °C (2 days), and (c) 34 °C (7 days).

From our normal-mode analyses of PEO,[17] we found that all molecules have, in addition to the LAM, a LAM-like mode, viz., a mode that exhibits obvious LAM characteristics in its atomic displacements. We showed that its frequency is about half that of the LAM and that its intensity varies with the chain length, with a maximum in the vicinity of PEO 1000. On this basis, the band at 8.1 cm^{-1} can confidently be assigned to the LAM-like vibration of PEO 1000. Lower, though observable, intensity is expected for PEO 1500, and in fact a weak band is observed near 6 cm^{-1} in its spectrum (Figure 3a) that can be assigned to this mode. Our calculations[17] show that the LAM-like mode again has significant intensity when a molecule becomes longer than PEO 2000. However, the LAM bands of these or higher molecular weight samples are observed below 10 cm^{-1}, and thus the corresponding frequencies of the LAM-like vibrations will be lower than 5 cm^{-1}, which is very close to the Rayleigh line. We thus expect that the LAM-like modes of such samples are superimposed on the wing of the Rayleigh line and will not be resolved.

DSC thermograms of PEO 1000 (Figure 8) show two melting peaks. The positions of both peaks and the intensity of the lower peak increase as crystallization temperature and time increase (Table III). The presence of two melting peaks is probably due to fractionation, as was the case for PEO 1500; this can also be perceived in the X-ray patterns in Figure 7, where a small peak and a shoulder are found near the strong reflection at $2\theta = 1.30°$. Evidence of fractionation is not seen in the LAM spectra, although two strong melting peaks are found for the $T_c = 34$ °C sample (Figure 8c). This is probably because the LAM bands corresponding to the segregated chains overlap the lattice mode near 19 cm^{-1}, making the kinds of effects seen for PEO 1500 (cf. Figure 3) difficult to observe.

The increase in melting temperature with T_c and time is probably related to the similar increase in LAM fre-

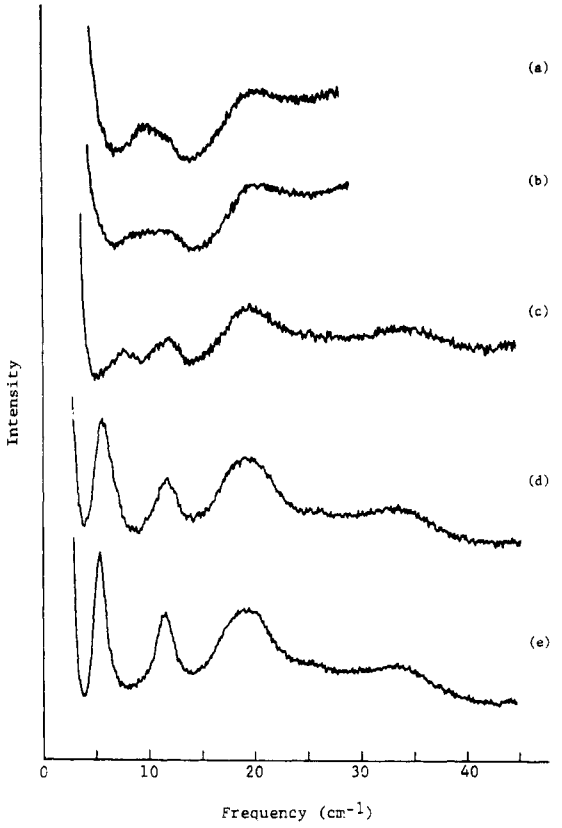

Figure 9. Low-frequency Raman spectra of PEO 3000 crystallized at different conditions: (a) RT (1 day), (b) RT (2 days), (c) RT (45 days), (d) 46 °C, and (e) 55 °C.

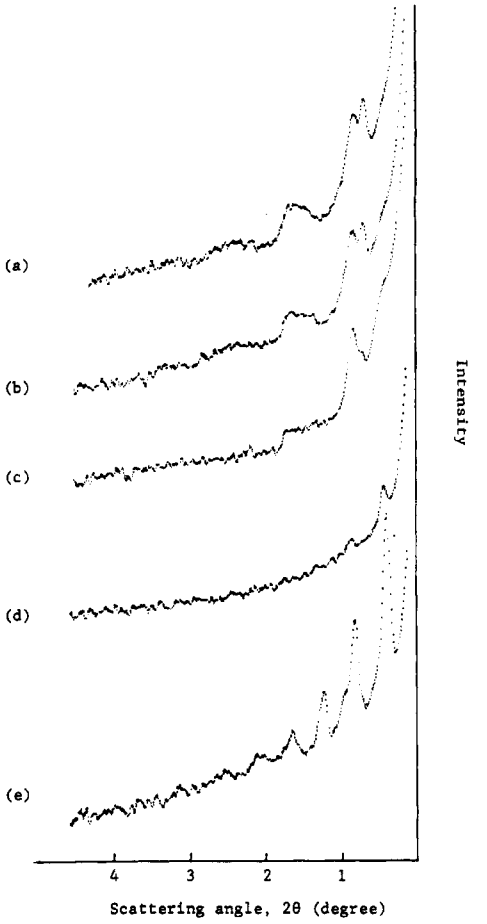

Figure 10. SAXS patterns of PEO 3000 crystallized at different conditions: (a) RT (1 day), (b) RT (2 days), (c) RT (45 days), (d) 46 °C, and (e) 55 °C.

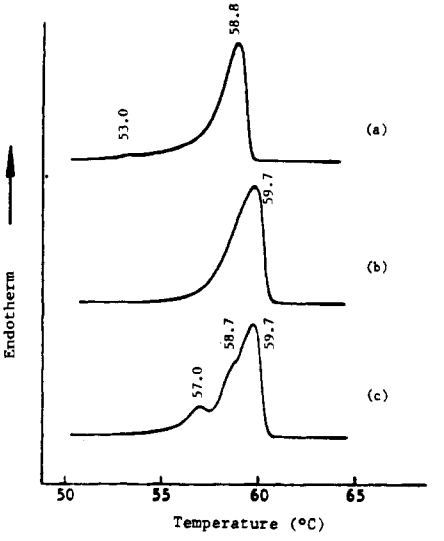

Figure 11. DSC melting curves of PEO 3000 crystallized at different temperatures: (a) RT (45 days), (b) 46 °C, and (c) 55 °C.

quency (Table III). Although the increase in LAM frequency might indicate a decrease in stem length, such a change is not consistent with the increase in melting temperature and is not expected to occur for higher T_c. The results of our normal-coordinate analyses[17] indicate that the LAM frequency is significantly affected by lateral interchain interactions. Thus, we believe that the increase in LAM frequency is more likely to be due to an increase in interchain interactions resulting from a perfection of crystal structure with increasing crystallization temperature and time. This can also account for the increase in melting temperature seen in the DSC thermograms.

Folded-Chain PEO. PEO 3000. In Figures 9 and 10 we show the low-frequency Raman spectra and SAXS patterns, respectively, of PEO 3000 samples crystallized at different conditions. We consider first the T_c = 55 °C sample. In addition to two lattice mode bands near 19.5 and 33.5 cm^{-1}, two intense peaks are found at 5.5 and 11.6 cm^{-1} in Figure 9e. We can assign both peaks to LAM bands based on the results of normal-mode calculations: the 5.5- and 11.6-cm^{-1} bands correspond to stem lengths of extended (E) and once-folded (F2: the number represents the number of stems) chain molecules, respectively. (The band at 11.6 cm^{-1} cannot be assigned to LAM-3 of the 5.5-cm^{-1} band, since its ratio (2.1) is too low, and in any case it can appear without the 5.5-cm^{-1} band, as in Figure 9c). X-ray diffraction maxima for this sample are clearly seen up to the fifth order of a periodicity of 214 Å (Figure 10e), which is equal to the length of E chains (Table IV). Since the Raman spectrum shows a LAM band corresponding to F2 chains, it might be thought that such stacked monolayer, F2(M), lamellae are also represented in the X-ray diffraction pattern, since the second-order reflection of E lamellae could overlap the first-order peak of F2(M) lamellae. But this possibility is not likely, since the intensities of the Bragg reflections shown in Figure 10e decrease smoothly as the reflection order increases, as expected for the presence of a single structural periodicity corresponding to E lamellae.

This conclusion is also supported by DSC data (Figure 11c). The T_c = 55 °C sample does not show a peak near the expected[8,9] melting temperature of 53 °C for F2(M) lamellae, consistent with other studies[4,9] on a sim-

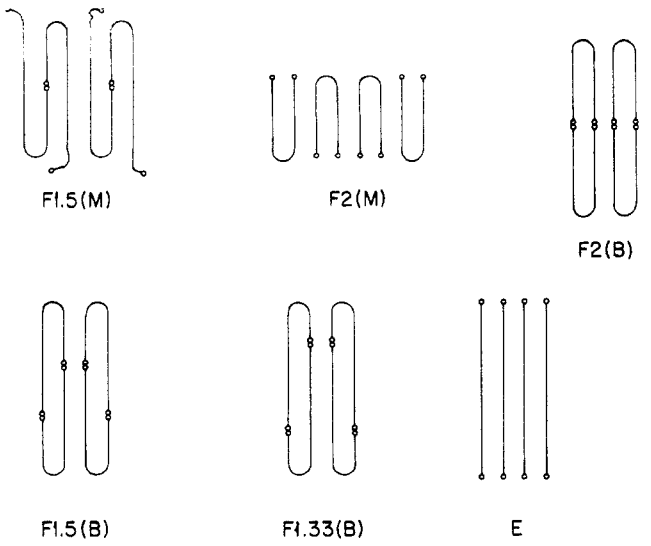

Figure 12. Schematic models of chain-folded and extended structures.

ilar molecular weight sample, which show that such lamellae are not expected for this T_c. (On the other hand, for a T_c = RT sample, Figure 11a, we do find a small 53 °C melting peak, which (see below) is clearly assignable to F2(M) lamellae.) Therefore, we believe that the only consistent explanation of these data is that the F2 chains are present in bilayer, F2(B), arrangements (see Figure 12). Such lamellae have about the same thickness as E lamellae and, if interspersed among them, would not interfere with the observation of a SAXS spacing corresponding to extended chains. The shoulder at 58.7 °C (Figure 11c) can in fact be assigned to F2(B) lamellae (see below; the 57.0 °C peak is probably a result of fractionation at this high T_c), while the 59.7 °C peak has been associated[8,9] with lamellae of E chains. However, in view of the relative intensity of the 11.6-cm^{-1} band in the Raman and the weak shoulder at 58.7 °C in the DSC, the possibility should not be excluded that F2(B) chain structures are present within E lamellae (see Figure 13). We return to this point later and also when discussing the PEO 5000 samples.

Features similar to those of the T_c = 55 °C sample are observed for the T_c = 46 °C sample in the LAM spectrum (Figure 9d) and in the X-ray diffraction pattern (Figure 10d), although in the latter case fewer orders are seen. However, the DSC curve for this sample shows only one peak (Figure 11b) that is asymmetrically broadened on the low-temperature side. The main melting peak, at 59.7 °C, is the same for both samples. The shoulder seen at 58.7 °C for the T_c = 55 °C sample is probably also present in the broad asymmetric peak at 59.7 °C of the T_c = 46 °C sample. We therefore believe that the lamellar structures are essentially similar at both crystallization temperatures.

The sample crystallized at room temperature, investigated at three different crystallization times (t_c), gives quite different results. The three X-ray scattering curves displayed at the top of Figure 10 (a–c) are for the T_c = RT samples crystallized for 1, 2, and 45 days, respectively. For t_c = 1 day there are reflections at 2θ = 0.69° (128 Å) and 0.82° (107 Å), with their weak second-order reflections near 2θ = 1.5°. As t_c increases, the intensity of the 128-Å peak decreases, becoming a shoulder for t_c = 45 days, while the 107-Å peak increases in intensity to become prominent for the t_c = 45 days sample. Also, a shoulder at 2θ = 0.41° (214 Å) becomes more noticeable

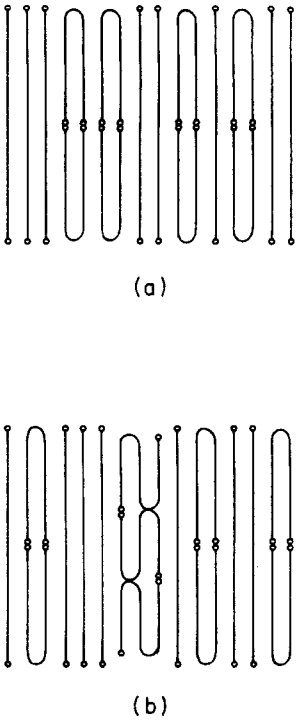

Figure 13. Schematic models of mixed-integer-fold lamellae: (a) E + F2(B), (b) E + F2(B) + F3(T).

Table IV
LAM Frequencies, X-ray Spacings, and Calculated Stem Lengths for Various Chain Models of PEO 3000

	LAM				
sample	obsd ν, cm^{-1}	calcd L,[a] Å	SAXS L, Å	chain model[b]	calcd stem L,[c] Å
T_c = RT (1 day)	9.5	122	128	F1.5(M)	135[d]
	11.6	102	107	F2(M)	101
T_c = RT (2 days)	11.6	102	214	F2(B)	2 × 101
	8.6	135	214	F1.5(B)	135 + 68
	9.5	122	128	F1.5(M)	135
	11.6	102	107	F2(M)	101
T_c = RT (45 days)	11.6	102	214	F2(B)	2 × 101
	7.5	153	214	F1.33(B)	152 + 51
	11.6	102	107	F2(M)	101
T_c = 46 °C	5.5	204	214	E	211
	11.6	102		F2(B)	2 × 101
T_c = 55 °C	5.5	204	214	E	211
	11.6	102		F2(B)	2 × 101

[a] Obtained from the plot in Figure 1. [b] (M) represents monolayer, (B), bilayer. [c] Calculated stem lengths within lamella, using eq 1; 8.3 Å is assumed for each fold in calculations of stem lengths for folded-chain molecules. Contribution of folds to lamellar thickness is not included. [d] Based on a "perfect" F1.5 structure.

as t_c increases. The 214- and 107-Å reflections correspond to spacings for E and F2(M) lamellae, respectively (see Table IV); these peaks cannot be assigned to the first- and second-order reflections of E lamellae because the first-order reflection is hardly observed for the t_c = 1 day sample and no third-order reflection is seen. The 128-Å periodicity is significantly different from the calculated lengths of E (211 Å) and F2 (101 Å) chains. As we discuss below, we think this spacing can be identified with F1.5(M) chains (see Figure 12).

The LAM spectra for the T_c = RT samples also show the effect of crystallization time. For the t_c = 1 day sample (Figure 9a), there appear to be at least two bands, one near 9.5 cm^{-1}, corresponding to a stem length of 122 Å, and another near 11.6 cm^{-1}, corresponding to a stem length of 102 Å (see Table IV). For the t_c = 2 day sample (Figure 9b) the situation is more complex and could

be represented by the superposition of the above two bands plus a band centered near 8.6 cm^{-1}. The latter corresponds to a stem length of 135 Å, for which there is no definable SAXS spacing. We consider below the interpretation of this peak. After t_c = 45 days (Figure 9c), essentially only two bands are seen, one at 11.6 cm^{-1} and another at 7.5 cm^{-1}, corresponding to a stem length of 153 Å. The 11.6-cm^{-1} band, corresponding to F2 chains, is observed for all T_c = RT samples and increases its intensity with t_c. This finding is consistent with the SAXS data, in which the increasingly intense 107-Å periodicity corresponds to F2(M) lamellae. The decrease in the 9.5-cm^{-1} band with t_c correlates with the decreasing intensity of the 128-Å periodicity in the SAXS. Since 9.5 cm^{-1} corresponds to a stem length of about this value, we believe that these LAM and SAXS data are consistent with F1.5(M) lamellae. (The LAM band of the shorter stem of the F1.5 molecule is expected to appear near 19 cm^{-1} and would be overlapped by the broad lattice mode peak at 19.5 cm^{-1}.) Note that a "perfect" F1.5 molecule of PEO 3000 would be expected to have a long-stem length of 135 Å. The observed data would thus indicate that a 10–20-Å length of the chain is not incorporated in the lamella, probably being in disordered chain ends ("cilia") and/or loose folds.

The observed DSC curve for the T_c = RT (t_c = 45 days) sample, shown in Figure 11a, has a very small endotherm peak near 53 °C (corresponding to F2(M) lamellae) and a strong melting peak at 58.8 °C. It has been reported[8] that a DSC melting peak of F2(M) lamellae for PEO 3000 is hardly detected due to rapid transformation of this structure during heating. We therefore expect that unstable F2(M) lamellae are transformed into a more stable structure during heating in the DSC and consequently show up in the scan only as a very small contribution. The strong DSC peak is mostly a result of this rearrangement and is believed to be due mainly to F2(B) molecules. This peak is also found in the high T_c samples as a shoulder. The main endotherm peak at 59.7 °C for the high T_c samples can thus be attributed to the melting of lamellae containing mostly E molecules.

These results can explain what is at first sight puzzling in the observed data for the T_c = RT samples, viz., the presence of an E spacing (214 Å) in the X-ray patterns but the clear absence of the corresponding LAM band (5.5 cm^{-1}) in the Raman spectra. If we suppose that the E spacing is associated with the structure of F2(B) chains, then the observed Raman (11.6 cm^{-1}) and SAXS (107 and 214 Å) data are consistent with the presence of F2(M) and F2(B) lamellae, respectively, in the T_c = RT samples. The additional bands at 8.6 cm^{-1} (t_c = 2 days) and 7.5 cm^{-1} (t_c = 45 days) correspond to spacings (135 and 153 Å, respectively) that are not seen in SAXS. The former is consistent with a perfect F1.5 chain and the latter with an F1.33 chain (see Figure 12). We must now ask whether the existence of these various structures is reasonable, perhaps implying chain transformations that accompany crystallization as a function of temperature and time.

The Raman, SAXS, and DSC data indicate that transient structures form during various stages of crystallization and that these can lead to the stable structures finally seen. There also seems to be a unique stage that precedes final conversion to an extended chain. In the T_c = RT, t_c = 1 day sample we see ordered lamellae of F2(M) chains as well as the less ordered F1.5(M) structures (see Table IV). The latter may be an intermediate stage in the development of F2(B) structures, which

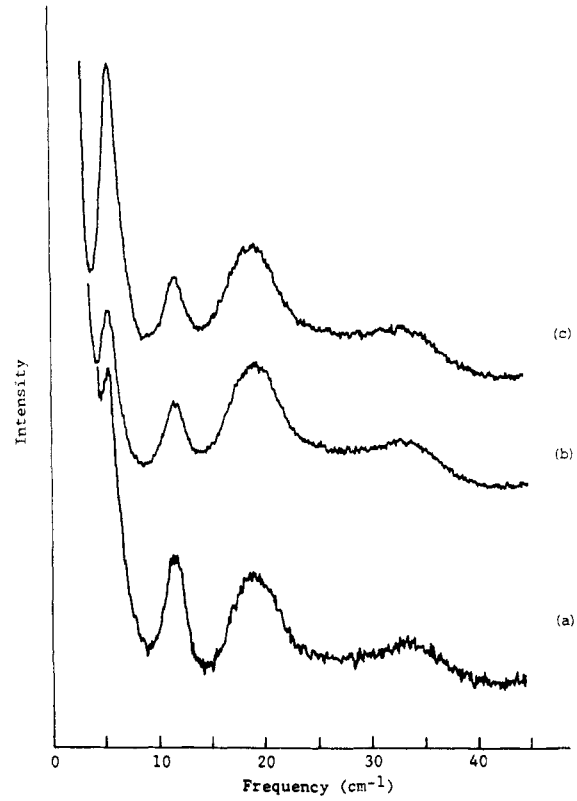

Figure 14. Low-frequency Raman spectra of PEO 3000 (T_c = RT sample) annealed at different temperatures: (a) 38 °C, (b) 47 °C, and (c) 55 °C.

are seen at t_c = 2 days and would be a reasonable way of initially reducing the number of conformational defects within the crystal. This transformation might occur by the less ordered F1.5(M) structure converting to ordered F2(M) lamellae, in which chain ends are now completely excluded from the crystal interior, followed by lateral reorganization of chains within a lamella to give F2(B) structures. Once an ordered F2(B) lamella is formed, reptation through F1.5(B) and F1.33(B) structures to the E state can occur without significant change in lamellar thickness. There may be nothing unique about these intermediate structures; i.e., the range between F2(B) and F1.33(B) may be continuous (as is perhaps indicated by the character of the LAM bands in parts a and b of Figure 9). On the other hand, structures beyond about F1.33(B) may be unstable and convert directly to E. This is supported by the results of annealing such a sample at elevated temperatures, T_a (Figure 14): at T_a = 38 °C the 7.5-cm^{-1} band disappears and a 5.5-cm^{-1} band appears, which increases in intensity as T_a increases. It is interesting that at T_a = 55 °C we still see a band at 11.6 cm^{-1}, associated with F2 chains. Thus, at high T_c, as DSC shows, we see only some residual untransformed F2(B) lamellae and the final E lamellae, probably with some F2(B) chains incorporated.

It is interesting to note that our normal-mode analyses[18] predict that, regardless of its conformation, the presence of a fold results in only a small decrease in the LAM frequency but a significant decrease in the LAM intensity. This prediction is in agreement with our findings. The position of the observed LAM frequency (11.6 cm^{-1}) of an F2 chain of PEO 3000 falls consistently between those of E chains of PEO 2000 (9.5 cm^{-1}) and PEO 1500 (13.2 cm^{-1}), as expected from calculated stem lengths of 101, 124, and 90 Å, respectively. However, the intensity of the LAM band for F2 chains of PEO 3000 is much weaker than those of LAM bands for E chains of PEO

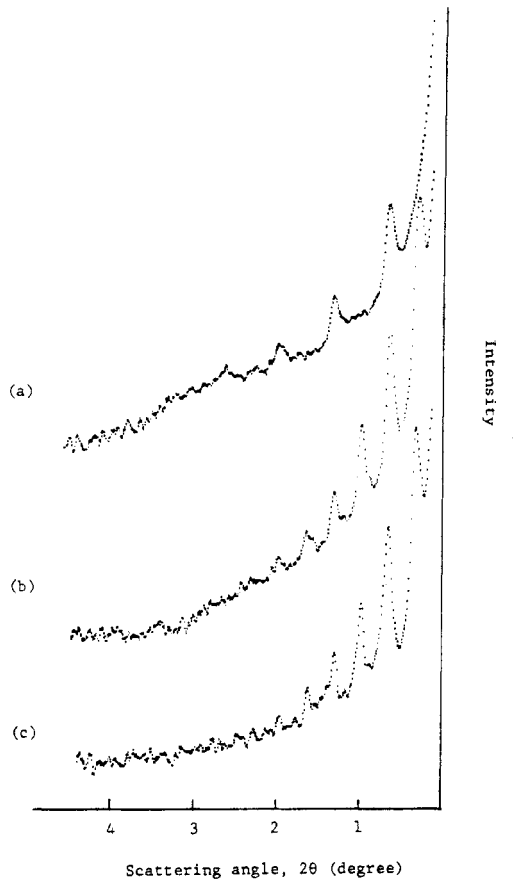

Figure 15. Small-angle X-ray diffraction patterns of PEO 5000 crystallized at different temperatures: (a) RT, (b) 46 °C, and (c) 58 °C.

Table V
LAM Frequencies, X-ray Spacings, and Calculated Stem Lengths for Various Chain Models of PEO 5000

sample	LAM obsd ν, cm^{-1}	LAM calcd L,[a] Å	SAXS L, Å	chain model[b]	calcd stem L,[c] Å
T_c = RT	8.5	136	136	F2(M)	138
T_c = 46 °C	8.7	133	269	F2(B)	2 × 138
T_c = 58 °C	3.9	274	273	E	285
	8.7	133		F2(B)	2 × 138
	13.5	88		F3(T)	3 × 89

[a] Obtained from the plot in Figure 1. [b] (M) represents monolayer, (B) bilayer, and (T) trilayer. [c] Calculated stem lengths within lamella, using eq 1; 8.3 Å is assumed for each fold in calculations of stem lengths for folded-chain molecules. Contribution of folds to lamellar thickness is not included.

2000 and PEO 1500, when compared to the lattice mode band at 19.5 cm^{-1}.

PEO 5000. In Figure 15 we present the SAXS patterns of PEO 5000 crystallized at different temperatures. X-ray periodicities corresponding to E chains (~270 Å) are observed for T_c = 46 °C and T_c = 58 °C samples, while the T_c = RT (t_c = 10 days) sample shows a periodicity of 136 Å, consistent with F2(M) chains (see Table V). For the T_c = RT sample, the Raman spectrum (Figure 16a) has a band at 8.5 cm^{-1}, corresponding to a stem length of 136 Å, and the DSC curve (Figure 17a) shows two melting peaks, at 58.3 and 61.2 °C. Since only the F2 lamellar spacing is found in the X-ray pattern for the T_c = RT sample, the Raman band at 8.5 cm^{-1} can be unambiguously assigned to the LAM of F2(M) chains. This may make the appearance of two melting peaks in the DSC seem strange. However, this would be expected if structural transformation occurs during heating in the

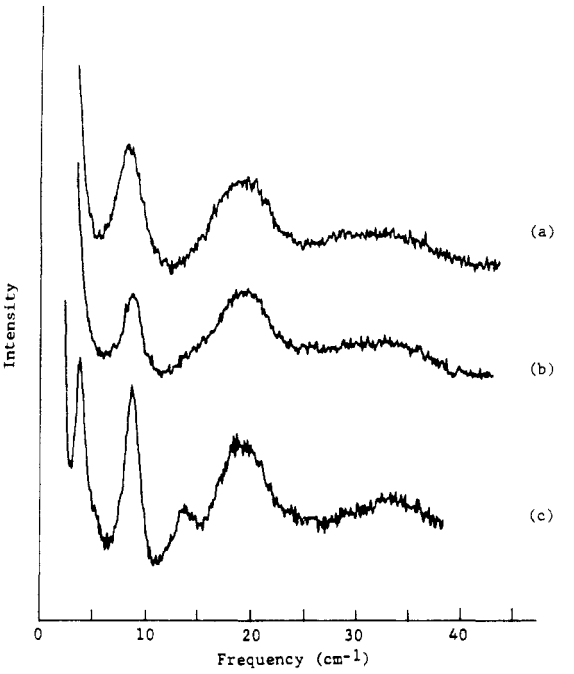

Figure 16. Low-frequency Raman spectra of PEO 5000 crystallized at different temperatures: (a) RT, (b) 46 °C, and (c) 58 °C.

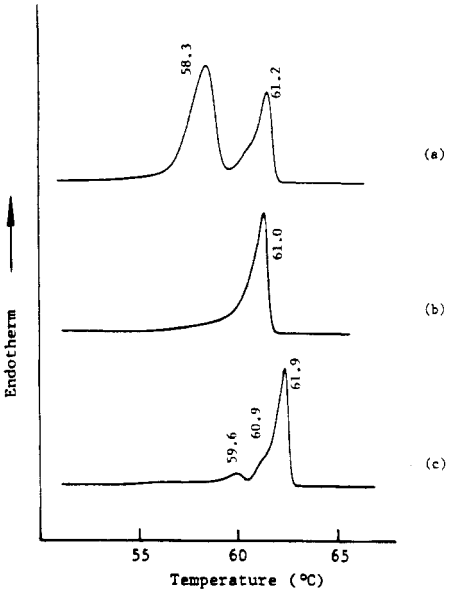

Figure 17. DSC melting curves at a heating rate of 5 °C/min for PEO 5000 crystallized at different temperatures: (a) RT (10 days), (b) 46 °C, and (c) 58 °C.

DSC, in which case we expect to observe two distinct melting peaks with a different ratio of peak areas as the heating rate changes. This is in fact the case when this sample is heated at the slower rate of 0.5 °C/min (Figure 18a): the area of the higher temperature endotherm peak (which shifts to 60.9 °C) increases dramatically at the expense of the lower temperature peak. Therefore, the lower melting peak corresponds to an F2(M) structure that is unstable on heating in the DSC, the higher melting peak being a result of reorganization of this structure during heating, most likely to an F2(B) structure. An exothermic peak corresponding to the reorganization is not seen in the DSC thermograms. This can be ascribed to the occurrence of simultaneous melting and recrystallization processes, as was indicated by Kovacs et al.[8]

We should note that the T_c = RT sample also shows time-dependent effects,[25] though these are different from

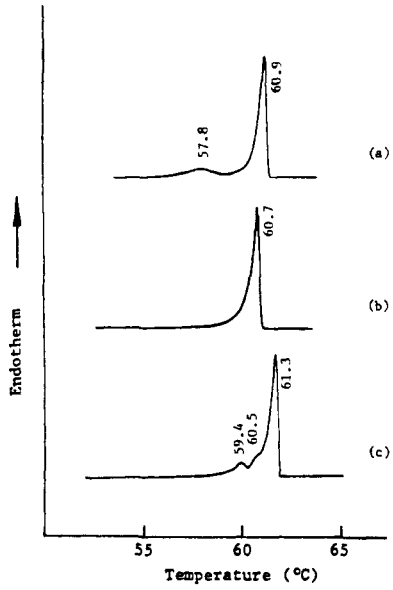

Figure 18. DSC melting curves at a heating rate of 0.5 °C/min for PEO 5000 crystallized at different temperatures: (a) RT (10 days), (b) 46 °C, and (c) 58 °C.

what was seen for the PEO 3000 sample. As t_c increases, the LAM peak shifts to higher frequency, as do the DSC melting peaks accompanied by a decrease in the relative area of the lower temperature peak. We think that both of these observations are consistent with an increase in order of the F2(M) lamellae with time, with a possible conversion of some to F2(B) lamellae.

For the T_c = 58 °C sample, the Raman spectrum (Figure 16c) shows three peaks, at 3.9, 8.7, and 13.5 cm^{-1}. The results of normal-coordinate analyses (Figure 1) indicate that these three bands can be assigned to the LAM of E, F2, and F3 molecules, respectively (see Table V). The SAXS pattern of this sample (Figure 15c) shows at least 6 orders of a periodicity corresponding to E chains. The DSC curve for this sample (Figure 17c) shows a strong peak at 61.9 °C, a shoulder at 60.9 °C, and a small peak at 59.6 °C. The small peak is probably a result of fractionation that is observed when crystallization occurs near the melting point, as seen for other PEO samples. The shoulder at 60.9 °C, which is found for the other samples as a prominent peak, is consistent with a minor amount of F2(B) lamellae. The strong peak at 61.9 °C, which is 1 °C higher than the shoulder, probably corresponds to lamellae having mainly E chains. By comparison with the DSC curve at the lower heating rate (Figure 18c), we can infer that the structures corresponding to these melting peaks do not transform during DSC heating but remain stable until completion of their melting. The observation of three LAM bands corresponding to E, F2, and F3 chains, the presence of only the E spacing in the X-ray pattern, and the absence of melting peaks for F2(M) chains (observed at 58.3 °C for the T_c = RT sample) and F3(M) chains in the DSC thermogram, indicate that a single major species is present in which F2 and F3 chains can exist in bilayer and trilayer arrangements together with E chains (see Figure 13). This is supported by the results of annealing studies:[25] even at T_a = 59 °C, LAM bands due to F2 and F3 chains are still present.

For the T_c = 46 °C sample, a periodicity corresponding to E chains is found in the X-ray pattern (Figure 15b) and a LAM band at 8.7 cm^{-1}, corresponding to F2 chains, is observed in the Raman spectrum (Figure 16b). The DSC melting curve for this sample (Figure 17b) has a single peak at 61.0 °C. The absence of a peak corresponding to F2(M) chains, the observation of the LAM band of F2 chains, and the presence of only an E spacing in SAXS suggest that F2 chains occur in bilayer arrangements. Therefore, the absence of a melting peak at 61.9 °C, associated with E lamellae for the T_c = 58 °C sample, indicates that F2(B) lamellae are the principal species present in the T_c = 46 °C sample.

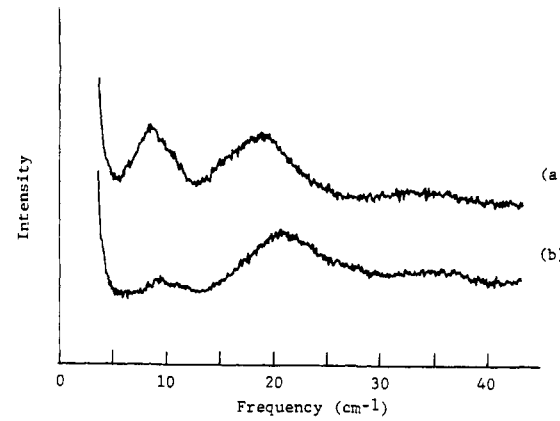

Figure 19. Low-frequency Raman spectra of PEO 1000 [T_a = 34 °C (7 days)] recorded at (a) +25 °C and (b) −79 °C.

As we have seen for the T_c = 58 °C sample, the strong F2 LAM band at 8.7 cm^{-1}, and the significant F3 LAM band at 13.5 cm^{-1}, the single pronounced periodicity of approximately E chain length in the SAXS, the negligible amount of F2(B) lamellae, and absence of F3(M) lamellae in the DSC are consistent with the existence of mixed lamellae, viz., the single species in which all three chain structures are present (Figure 13). The SAXS data seem to provide other evidence for the existence of such mixed lamellae. As seen in Table V, the observed X-ray spacing for the T_c = 58 °C sample (273 Å) is ~10 Å shorter than the calculated length of an E chain (285 Å). The thickness of F2(B) and F3(T) lamellae should be smaller than that of an E lamella since a few units are assigned to the folds. If we assume three chemical repeat units for each fold, corresponding to 8.3 Å in the chain axis direction, the stem thicknesses of an F2(B) lamella and an F3(T) lamella are 8.3 and 16.6 Å, respectively, smaller than the chain length of an E chain. Considering the thickness of a fold itself to be a few angstroms, the observed X-ray periodicity for the T_c = 58 °C sample is consistent with the thickness of an F3(T) lamella, thus providing independent evidence for the existence of such mixed-integer lamellar structures. In such a structure, the E chains will have disordered ends outside the lamella and the F2 chains may have slightly irregular folds.

Temperature Dependence of LAM. By examining the effects of temperature on the LAM frequency and intensity through normal-mode analyses,[17] we are able to gain another perspective on the characteristics of this mode and to evaluate the validity of our assumptions about the importance and magnitudes of interaction forces that influence its behavior. It is therefore useful to compare these predictions[17] with experimental results.

In addition to room temperature, the LAM spectra of PEO 1000 through PEO 5000 were investigated at the temperature of a dry ice/acetone mixture. We have already shown the results for PEO 2000 in Figure 2. The low-temperature LAM spectrum of PEO 1000 (Figure 19) exhibits similar changes in frequencies and intensities. The frequency increase and the intensity decrease are obvious for the LAM-like band at 8.6 cm^{-1}. For the LAM band at 19.2 cm^{-1}, only the frequency shift is clearly seen because it superimposes on the lattice mode peak near

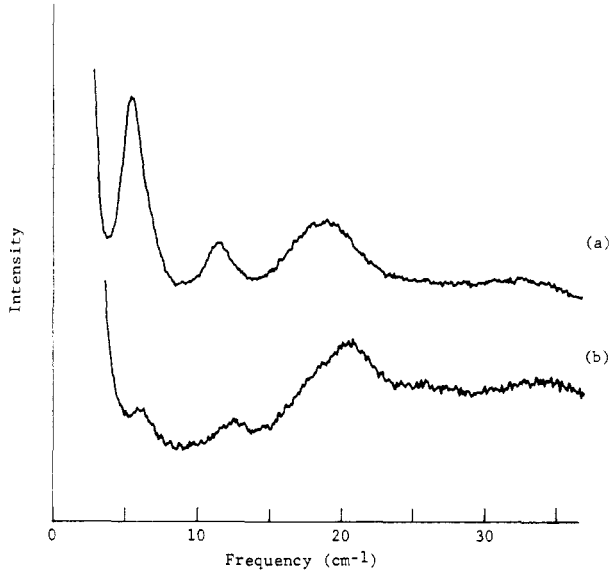

Figure 20. Low-frequency Raman spectra of PEO 3000 (T_a = 55 °C) recorded at (a) +25 °C and (b) −79 °C.

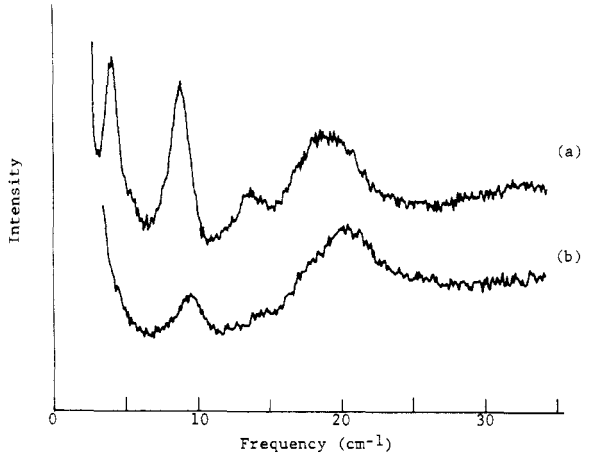

Figure 21. Low-frequency Raman spectra of PEO 5000 (T_c = 58 °C) recorded at (a) +25 °C and (b) −79 °C.

19.5 cm^{-1}, whose intensity should not change significantly at the lower temperature. In Figure 20 are shown the LAM spectra of PEO 3000 recorded at room temperature and at the low temperature. Both LAM bands show frequency and intensity changes on cooling. The intensity decrease is much more significant for the 5.5-cm^{-1} band, corresponding to E chains, than for the 11.6-cm^{-1} band, corresponding to F2 chains. Such changes in intensities are also found in the LAM spectra of PEO 5000 (Figure 21). The 3.9-cm^{-1} band, due to E chains, seems to disappear in the low-temperature spectrum, although this change might be difficult to detect because of the experimental problem in resolving a peak below 5 cm^{-1} as well as the decrease in intensity upon cooling. The 8.7-cm^{-1} band, corresponding to F2 chains, shifts to 9.6 cm^{-1} and weakens but still retains considerable intensity. The weak 13.5-cm^{-1} band, due to F3 chains, weakens but is still visible near 15 cm^{-1} in the low-temperature spectrum. These changes with temperature are completely reversible for the PEO 3000 sample. For the PEO 5000 sample, a 3.9-cm^{-1} band is seen again when the sample is brought back to room temperature, although its intensity is somewhat lower compared to the 8.7-cm^{-1} band. The frequency changes are tabulated in Table VI.

The frequency increase at the lower temperature can be easily understood. The interchain separation decreases upon cooling due to thermal contraction of the unit cell, thus increasing the intermolecular forces. Our normal-mode calculations[17] indicate that the LAM frequency increases with intermolecular forces, such as hydrogen bonding at chain ends and lateral van der Waals interchain interactions. The observed increases in frequencies with decreasing temperature have about the same ratio for all samples (Table VI) because they share the same crystal structure. This increase, ~10%, is also predicted by our calculations of such temperature effects[17] and is much larger than that for planar zigzag polyethylene.[32,33] This is one of the arguments supporting our contention that the LAM in helical chains is much more sensitive to lateral interchain interactions than that in planar zigzag chains.

Table VI
Observed LAM Frequencies of PEO as a Function of Temperature

sample	frequency, cm^{-1} T = 25 °C	T = −79 °C	frequency ratio
1000	8.6	9.6	1.12
2000	9.5	10.5	1.11
3000	5.5	6.1	1.11
	11.6	12.6	1.09
5000	3.9		
	8.7	9.6	1.10
	13.5	15.0	1.11

A change in observed Raman intensity with temperature is expected since the correction term[23] for the theoretical intensity contains a temperature factor. However, such a correction (ca. 30%) cannot account for the significant intensity decrease observed for the LAM bands of PEO. As pointed out in our normal-mode calculations,[17] the LAM intensity is affected by the changes in end and lateral interchain interactions. The intensity changes are mostly dependent on the interactions at the chain ends, with the LAM intensity expected to decrease as such interactions at the chain ends increase on cooling. In order to check this general effect, the LAM spectrum of PEO 3000 was studied above room temperature. Indeed, at 48 °C we observed frequency decreases, the 5.5- and 11.6-cm^{-1} bands shifting to 5.0 and 11.0 cm^{-1}, respectively, and intensity increases, as expected at the higher temperature. Thus, the LAM intensity changes on cooling or heating can be explained in terms of the changes in interchain interactions as the unit cell contracts or expands.

As we have noted, larger intensity decreases are observed at the lower temperature for the LAM bands of E chains than for those of F2 chains. This is due to the difference in end interactions for these two kinds of molecules. Since the E chain may be hydrogen bonded at both ends, it is susceptible to larger changes in the end force interactions than is the F2 chain, which has a fold at one end. As we have shown,[17] the intensity is affected much more by small changes in weak end forces than by small changes in already existent lateral interactions. Thus, the observed behavior of the LAM frequencies and intensities with temperature are in good agreement with the results of our normal-mode calculations and help to validate our assumptions about the influence of interchain interactions on the LAM of helical chains.

Conclusions

By incorporating an analysis of Raman LAM spectra with SAXS and DSC studies of PEO, we have been able to extend the insights gained from the previous applications of the latter two techniques.[1-9] This was made pos-

sible by the detailed understanding of the LAM in this helical polymer achieved through normal-mode calculations.[17,18] Not only has this approach enabled us to assign LAM bands unambiguously, but it has thereby permitted us to properly identify lattice modes of the crystal. For PEO 1000 and PEO 1500, we have observed a LAM-like mode in addition to the LAM, as predicted from our calculations. Fractionation of samples crystallized near the melting point was observed in the DSC of PEO 1500, and evidence of this was clearly seen in the LAM spectra. Such fractionation is also found for other samples. We observed for the first time the LAM bands corresponding to extended chains of PEO 3000 and PEO 5000.

The LAM spectra of certain samples of PEO 3000 clearly show the presence of F2 as well as E chains, and in the case of PEO 5000 both F2 and F3 chains can be present in addition to E chains. The SAXS and DSC data do not indicate that these exist as independent lamellae, and we are therefore led to suggest that mixed-integer lamellae are present, i.e., lamellae in which E as well as F2(B) chains (for PEO 3000) and E + F2(B) + F3(T) chains (for PEO 5000) coexist in the same lamella. This proposal is supported by the observation that prolonged annealing does not remove from the LAM spectra the bands associated with folded chains.

In the case of a T_c = RT PEO 3000 sample, we see a time-dependent LAM spectrum that provides insights into structural changes that can take place with crystallization. In the early stages, F1.5(M) and F2(M) lamellae are present (at this point we are not sure if one is the precursor of the other); with time, the former disappear and F2(B) lamellae become stabilized, with indications of the presence of F1.5(B) structures; at longer times, we see the presence of F1.33(B) structures, which presumably result from F2(B) and F1.5(B) structures by reptation. The latter process provides a reasonable mechanism for the final stage of conversion of once-folded to extended chains. The existence of F1.5(M) lamellae, though they are somewhat imperfect, would be consistent with the development of structures that minimize the number of chain ends ("defects") embedded in the crystal lattice.

These studies show that LAM spectra are needed if we are to infer aspects of internal structure in lamellae of PEO; SAXS plus DSC can provide only a limited view of such details. For higher molecular weight samples the situation will be more complex, since more multifolded molecules are possible and therefore the LAM spectrum will contain a larger number of bands. We have already seen this for PEO 10 000,[25] for which an analysis is in progress. The LAM analyses will be crucial in obtaining complete characterizations of such systems.

Acknowledgment. This research was supported by the Polymers Program of NSF, Grant DMR-8806975, and by a fellowship from the Macromolecular Research Center to K.S.

References and Notes

(1) Arlie, J. P.; Spegt, P.; Skoulios, A. *Makromol. Chem.* **1967**, *104*, 212.
(2) Spegt, P. *Makromol. Chem.* **1970**, *139*, 139.
(3) Spegt, P. *Makromol. Chem.* **1970**, *140*, 167.
(4) Kovacs, A. J.; Gonthier, A. *Kolloid Z. Z. Polym.* **1972**, *250*, 530.
(5) Kovacs, A. J.; Gonthier, A.; Straupe, C. *J. Polym. Sci., Part C* **1975**, *50*, 283.
(6) Kovacs, A. J.; Straupe, C.; Gonthier, A. *J. Polym. Sci., Part C* **1977**, *59*, 31.
(7) Kovacs, A. J.; Straupe, C. *J. Cryst. Growth* **1980**, *48*, 210.
(8) Buckley, C. P.; Kovacs, A. J. *Kolloid Z. Z. Polym.* **1976**, *254*, 695.
(9) Cheng, S. Z. D.; Wunderlich, B. *J. Polym. Sci., Polym. Phys. Ed.* **1986**, *24*, 577.
(10) Ungar, G.; Stejny, J.; Keller, A.; Bidd, I.; Whiting, M. C. *Science* **1985**, *229*, 386.
(11) Cheng, S. Z. D.; Bu, H. S.; Wunderlich, B. *Polymer* **1988**, *29*, 579.
(12) Lee, K. S.; Wegner, G. *Makromol. Chem., Rapid Commun.* **1985**, *6*, 203.
(13) Ungar, G.; Keller, A. *Polymer* **1986**, *27*, 1835.
(14) Hsu, S. L.; Krimm, S. *J. Appl. Phys.* **1976**, *47*, 4265.
(15) Hsu, S. L.; Ford, G. W.; Krimm, S. *J. Polym. Sci., Polym. Phys. Ed.* **1977**, *15*, 1769.
(16) Chang, C.; Krimm, S. *J. Appl. Phys.* **1983**, *54*, 5526.
(17) Song, K.; Krimm, S. *J. Polym. Sci., Polym. Phys. Ed.* **1990**, *28*, 35.
(18) Song, K.; Krimm, S. *J. Polym. Sci., Polym. Phys. Ed.* **1990**, *28*, 51.
(19) Song, K.; Krimm, S. *Macromolecules* **1989**, *22*, 1504.
(20) Takahashi, Y.; Tadokoro, H. *Macromolecules* **1973**, *6*, 672.
(21) Blundell, D. J.; Keller, A.; Kovacs, A. J. *J. Polym. Sci., Part B* **1966**, *4*, 481.
(22) Bendtsen, J. *J. Raman Spectrosc.* **1974**, *2*, 133.
(23) Snyder, R. G.; Scherer, J. R. *J. Polym. Sci., Polym. Phys. Ed.* **1980**, *18*, 421.
(24) Marshall, A.; Domzy, R. C.; Teo, H. H.; Mobbs, R. H.; Booth, C. *Eur. Polym. J.* **1981**, *17*, 885.
(25) Song, K. Ph.D. Thesis, University of Michigan, Ann Arbor, MI, 1988.
(26) Viras, K.; Teo, H. H.; Marshall, A.; Domszy, R. C.; King, T. A.; Booth, C. *J. Polym. Sci., Polym. Phys. Ed.* **1983**, *21*, 919.
(27) Teo, H. H.; Marshall, A.; Booth, C. *Makromol. Chem.* **1982**, *183*, 2265.
(28) Rabolt, J. F.; Johnson, K. W.; Zitter, R. N. *J. Chem. Phys.* **1974**, *61*, 504.
(29) Viras, K.; King, T. A.; Booth, C. *J. Polym. Sci., Polym. Phys. Ed.* **1985**, *23*, 471.
(30) Arlie, J. P.; Spegt, P. A.; Skoulios, A. E. *Makromol. Chem.* **1966**, *99*, 160.
(31) Fraser, M. J.; Cooper, D. R.; Booth, C. *Polymer* **1977**, *18*, 351.
(32) Khoury, F.; Fanconi, B.; Barnes, J. D.; Bolz, L. H. *J. Chem. Phys.* **1973**, *59*, 5849.
(33) Olf, H. G.; Fanconi, B. *J. Chem. Phys.* **1973**, *59*, 534.

Registry No. PEO, 25322-68-3.